Proceedings of the 2007 IEEE
International Conference on Mechatronics and Automation
August 5 - 8, 2007, Harbin, China

Enhanced Sensitivity of Mass Detection Using the First Torsional Mode of Microcantilevers

Hui Xie, Julien Vitard, Sinan Haliyo, Stéphane Régnier

Robotics Laboratory
Pierre and Marie Curie University -Paris VI/CNRS
18 Route du Panorama - BP 61, 92265 FONTENAY-AUX-ROSES, France

xie@robot.jussieu.fr

***Abstract* - Using higher resonant modes of microcantilevers promises higher sensitivity in the bio/chemical molecular detection. Compared with the first flexure modes, the first torsional mode can provide an improved mass-sensing resolution due to the higher quality factor. For the accurate characterization of the torsional mode and further detection of the multi-mass attached to the microcantilevers, models based on the Rayleigh-Ritz method, considering the attaching positions of the micro and nano objects adhered to the microcantilevers is developed. An ragweed pollen, as target mass are located on different positions on a commercial microcantilever for the contrastive experiments of the first and second flexure and the first torsional resonances in the air. From experimental vibration spectrums of the "cantilever-object" system, we can get that the mass sensitivity of the torsional mode is an order higher than the conventionally used the first flexural mode. The torsional mode can offer significantly enhanced mass sensitivity within the realm of existing microcantilever technology.**

Index Terms – Mass detection, microcantilever, resonant frequency, the first torsional mode.

I. INTRODUCTION

Motivated by the need of high-sensitive mass detection of micro and nano-objects adhered to the microcantilever on different positions, we have conducted a dynamic model and method for the mass detection using the first torsional mode of Atomic force microscope (AFM) cantilevers. AFM, which has been brought into this world for more than two decades [1], has been proved to be a powerful tool in the research and application of the nanotechnology. Not only can it be used for the characterization of the micro and nano-samples, but also the nanofabrication through the manipulation. Recently, vigorous development of the nanotechnology provides the AFM more important roles in the research areas.

Among all the research work relating to the AFM cantilever, one particular kind of application is the high sensitivity mass detection by the measurement of resonant frequency shift before and after the load of the additional mass. An early example for the cantilever-mass system was used for the determination of the spring constant of AFM cantilevers by adding a known small mass on the tip of the cantilevers and then measuring their resonant frequency shift [2]. In contrast with the static method, utilizing the detection of resonant frequency shift of microcantilever can provide higher sensitivity allowing detection in the attogram regime. Gradually, the change in resonant frequency of the cantilever beam, due to the mass adhered to the cantilever, has been widely used as a detection scheme for the small mass. The theoretical sensitivity on the attogram scale of a mass sensor was demonstrated by a simple linear electromechanical model for an electrostatic driven resonating cantilever [3]. Several micro or nano-cantilevers based on the silicon microfabrication technology, with sensitivity from femtogram to attogram have been developed [4-9]. The highly sensitive and convenient micro and nano-cantilevers were widely used in the biology area, including the detection of DNA, virus and cells [10-13]. Based on both detection of frequency shift and bending of micro-cantilevers to measure mass changes as well as viscosity changes, novel designs for gas and liquid sensing were presented [14, 15]. As an extremely sensitive method, the Anderson or vibration localization was used in coupled microcantilevers to detect the added mass of a target analyte [16]. In [17], a dynamic method based on the Rayleigh-Ritz was introduced. Even the hot nanomaterial-carbon nanotube was also employed in this hot topic as a nanocantilever toward zeptogram detection [18]. In [19], it has been certified that the mass sensitivities of the torsional and lateral mode frequencies are an order of magnitude greater than that of the conventionally used fundamental bending mode. By positioning a single gold particle at different locations along the length axis on a cantilever based mass sensor, the fourth bending mode have been investigated has mass detection sensitivity [20]. Using a piezoresistive microcantilever, a resolution of tens-femtogram mass sensing in air has been obtained under the second flexural mode [21].

In this paper, the first torsional mode is used to achieve higher sensitivity of mass detection than the conventional flexural modes. A few researches paid attention to the adhering positions of the micro and nano-objects. Unless the mass is accurately fabricated on a special position on the cantilever, other methods for the mass absorbing, accurately placing and distributing will undoubtedly bring positioning errors to the mass loading. Therefore, in order to reduce the effect of the adhering position errors, a "cantilever-object" system model, based on the Rayleigh-Ritz method, considering the position of the multi-object adhered to the AFM cantilevers is proposed. In this method, all the dimensions of the microcantilever as well as the adhering position of micro and nano-objects are involved into the same model. Once the longitudinal and

transversal adhering positions of micro and nano-objects and the resonant frequency of cantilever are known, the mass of can be precisely determined by the first torsional mode.

In our research, theories and models are introduced in section II. In section III, experiments and results mainly including precisely mass measuring and adhering position detecting of microspheres are presented. Discussions and future work are presented in section IV.

II. Theories And Models

A. Model of the cantilever

As shown in Figure 1, the cantilever is built in at one end, free at the other end assumed to deform in the linear elastic range. *L, w*, and *h* are the length, width and the thickness of a rectangular cantilever, respectively. The coordinates are defined as follows: the origin is located on the centre of the cross section of the built-in end, the *x*-axis is along its length, and the *z*-axis and *y*-axis are along its thickness and the *y*-axis, respectively. The motion of the torsional vibrations of micro-cantilever is a function of *x* [22]:

$$GJ\frac{\partial^2(\theta,t)}{\partial x^2}=\rho I_p\frac{\partial^2(\theta,t)}{\partial t^2}+c\frac{\partial(\theta,t)}{\partial t} \tag{1}$$

where θ is the rotation angle, G is the shear modulus, ρ is the density of the cantilever, c is the coefficient of viscous damping, $I_p = (wh^3+w^3h)/12$ is the polar area moment of inertia and J is the torsional constant. To the cantilever with a rectangular section, J can be obtained by [23]

$$J\approx\frac{1}{3}wh^3\left[1-0.63\frac{h}{w}+0.052\left(\frac{h}{w}\right)^5\right] \tag{2}$$

The n^{th} torsional frequency is obtained by

$$\omega=\frac{(2n-1)\pi}{2L}\sqrt{\frac{GJ}{\rho I_p}},\quad n=1,2,\ldots \tag{3}$$

B. Rayleigh-Ritz method

For many years, hundreds of research articles and many books have appeared that use Rayleigh and Ritz methods to resolve natural frequencies of continuum systems (bars, beams, membranes, plates), calling it the ‘‘Rayleigh–Ritz method.” Although this was claimed that the present writer concludes that Rayleigh’s name should not be attached to the Ritz method, that is, the ‘‘Rayleigh–Ritz method’’ is an improper designation [24], the classic and perfect method will be employed to solve the natural frequencies of cantilever-object system in our research. In Rayleigh’ method, potential (U) and kinetic (T) energies of the torsional system are considered to calculate the nature frequency of the system. The maximum U_{max} and T_{max} are defined by:

$$U_{\max}=\frac{1}{2}\int_0^L GJ\left[\frac{\partial z(x)}{\partial x}\right]^2dx \tag{4}$$

$$T_{\max}=\frac{1}{2}\omega^2\int_0^L\rho I_p z^2(x)dx \tag{5}$$

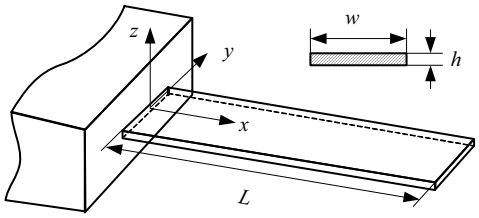

Fig. 1. The geometry model of the AFM cantilever

where ρ is the density and $z(x)$ is the function of the mode shape. In this method, by assuming the mode shape, and setting the maximum values of potential and kinetic energy in a cycle of motion equal to each other, therefore, to the continuum system, the nature frequency can be obtained by:

$$\omega^2=\frac{\int_0^L GJ\left[\frac{\partial z(x)}{\partial x}\right]^2dx}{\int_0^L\rho I_p z^2(x)dx} \tag{6}$$

It is very clear that the calculation accuracy strongly depends on how closely the assumed mode shape fits the exact one, especially to the system with multi-subsystems. In Ritz’s method, a displacement function is assumed in terms of a series of admissible displacement functions having undetermined coefficients, and then minimizes an energy functional involving U and T to determine frequencies and mode shapes. The mode function is defined by:

$$v(x)=\sum_{i=0}^{n}a_i\varphi_i(x) \tag{7}$$

where the $\varphi_i(x)$ is algebraic polynomials or trigonometric functions and the a_i are arbitrary coefficients, which is determined by partial derivatives of (6), for the calculation if the minimum frequency:

$$\frac{\partial\omega^2}{\partial a_i}=0\qquad(i=1,2,\cdots,n) \tag{8}$$

From the (6) and (7), a similar equation for the nature frequency is obtained:

$$\omega^2=\frac{\{a\}^T[K]\{a\}}{\{a\}^T[M]\{a\}}=\frac{\boldsymbol{K}}{\boldsymbol{M}} \tag{9}$$

where $\{a\}^T=\{a_1,a_2,\cdots,a_n\}$. According to the (9), the solution of the nature frequency is given by:

$$\left[\boldsymbol{K}-\omega^2\boldsymbol{M}\right]\{a\}=0 \tag{10}$$

so to the arbitrary coefficients {a}, the solution is:

$$\det(\boldsymbol{K}-\omega^2\boldsymbol{M})=0 \tag{11}$$

This is the famous Rayleigh–Ritz method for the calculation of the nature frequency of continuum systems. To a complex system consisting of multi-subsystems, for example the spring bearing and mass adhering to the vibrating continuum systems, the additional potential (U) and kinetic (T) energies should be added to the whole system. Therefore, in the “cantilever-object” system, adding the kinetic (T) energy of micro and nano-objects to the whole system, the nature frequency of the whole system can be accurately obtained.

C. Analysis for torsional vibration

The "cantilever-object" system is modelled in Figure 2. The torsional axis is along the x axis and through the centre of the cross section of the built-in end. In the first torsional model, three micro and nano-objects, adhering to the positions (l_x, l_y) has the mass of m, and two degrees of freedom t_1 and t_2, which are vertical to the x axis, are assigned to the system.

$$z_t(x) = t_1\psi_1(x) + t_2\psi_2(x) \tag{12}$$

where $\psi_1(x)$ and $\psi_2(x)$, the functions of the torsional angle, are x and x^2, respectively, t_1 and t_2 are two corresponding constants. So the maximum potential (U_t) and maximum kinetic (T_t) energies of the beam are given by:

$$U_t = \frac{1}{2}GJ\int_0^L\left[\sum_{i=1}^{2}t_i\frac{d\psi_i(x)}{dx}\right]\left[\sum_{j=1}^{2}t_j\frac{d\psi_j(x)}{dx}\right]dx \tag{13}$$

$$T_t = \frac{1}{2}\rho I_p\omega^2\int_0^L\left[\sum_{i=1}^{2}t_i\psi_i(x)\right]\left[\sum_{j=1}^{2}t_j\psi_j(x)\right]dx \tag{14}$$

where ρ is the density of cantilever, $I_p = (wh^3+w^3h)/12$ is the polar area moment of inertia, J is the torsional constant, which can be obtained by (2). So the factors of the matrix $\boldsymbol{K}$ and $\boldsymbol{M}$ for the torsional mode are given by:

$$k_{ij} = GJ\int_0^L\frac{\partial\varphi_i(x)}{\partial x}\cdot\frac{\partial\varphi_j(x)}{\partial x}dx \tag{15}$$

$$m_{ij} = \rho I_p\int_0^L\varphi_i(x)\cdot\varphi_j(x)dx \tag{16}$$

To the attaching objects, the elements are given by:

$$m_{ijobject} = \sum_{n=1}^{3}J_{mn}\psi_i(x)\cdot\psi_j(x) \tag{17}$$

where n is the number of the three micro and nano-objects and J_m is the inertia moment of mass. To the microsphere,

$$J_m = \frac{2}{5}mr^2 + m[l_{yn}^2 + (\frac{h}{2}+r)^2] \tag{18}$$

where r is the radius of the attaching object. So under the given coordinate system and [t_1, t_2], the mass matrix $\boldsymbol{M}$ and the stiffness $\boldsymbol{K}$ of the whole system are obtained by:

$$\boldsymbol{M} = \begin{bmatrix} \frac{1}{3}\rho I_p L^3 + \sum_{k=1}^{3}J_{mn}l_{xn}^2 & \frac{1}{4}\rho I_p L^4 + \sum_{k=1}^{3}J_{mn}l_{xn}^3 \\ \frac{1}{4}\rho I_p L^4 + \sum_{k=1}^{3}J_{mn}l_{xn}^3 & \frac{1}{5}\rho I_p L^5 + \sum_{k=1}^{3}J_{mn}l_{xn}^4 \end{bmatrix} \tag{19}$$

$$\boldsymbol{K} = \begin{bmatrix} GJL & GJL^2 \\ GJL^2 & \frac{4}{3}GJL^3 \end{bmatrix} \tag{20}$$

From (11), a solution in case of one object attached to the cantilever, including parameters of inertia moment J_m, resonant frequency ω and m, is obtained by:

$$f(l_{xn}, J_{mn}, \omega) = 0 \qquad (n = 1, 2, \cdots, N) \tag{21}$$

To the flexural mode, the similar equation can be obtained:

$$f(l_{xn}, m_n, \omega) = 0 \qquad (n = 1, 2, \cdots, N) \tag{22}$$

Note that in (21) there are four variables in this equation. l_{xn} is the longitude position of microspheres, and the inertia moment of mass J_{mn} is determined by the mass and the position of the object to the torsional axis. So if we know the resonant frequency of the "cantilever-object" system and the attaching positions of microspheres, the mass can be calculated.

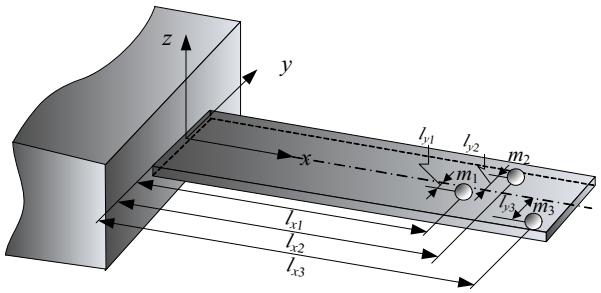

Fig. 2. The geometry model of the "cantilever-object" system. Three microspheres m_1, m_2 and m_3 attaching on the cantilever have coordinates of (l_{x1}, l_{y1}), (l_{x2}, l_{y2}) and (l_{x3}, l_{y3}), respectively.

III. Experiments And Results

A. Set-up of micromanipulator

The experimental micromanipulator consists of a support, a microcantilever, a piezoceramic and a laser beam deflection system. Generally, due to the fabrication errors, the spring constant of the cantilever varies from others fabricated on the different chips. As the cube of the thickness and length, and as a result dimensional errors induce large errors on the spring constant. Thus, accurate force calibration should be required for the characterization of each cantilever. In our research, the spring constant and thickness of three cantilevers are accurately calibrated.

The PI-89 piezoceramic has a thickness of 1 mm and 5mm and 8mm in width and length, respectively. Experimental results indicate that this piezoceramic has a fine linear relation between voltage input and displacement output, from 0-60nm under the input from 0-300V. A signal generator has been used to actuate the piezoceramic, which can produce sine waves ranging from 0 to 20 V, with bandwidth ranging from 1 to 3MHz and accuracies of 1 Hz from 0 to 10 kHz, 10 Hz below 1MHz, 100 Hz within the range of 1M-3MHz.

B. Calibration of cantilever

The scientific community needs a rapid and reliable way of accurately determining the stiffness of AFM cantilevers. Many methods, including the dynamic method (forced and thermal oscillation), static loading and FEA methods were widely used to calibrate the stiffness of the cantilever [25]. In [26], a hybrid method is introduced for the calibration of the spring constants of atomic force microscopy cantilevers. To the proposed method, the key parameters of the cantilever are the thickness h and the first torsional resonant frequency of the cantilever. If the first resonant frequency of the cantilever is determined, the thickness of the cantilever can be easily obtained.

The experimental cantilevers have wedge-shaped tip as in Fig. 3(b), in order to take into account the effect of wedge-shaped tip of the cantilever, the (4) and (5) should be modified for the flexural model:

$$k_{ij} = EI_y \int_0^{L-l_w} \frac{\partial^2 \varphi_i(x)}{\partial x^2} \cdot \frac{\partial^2 \varphi_j(x)}{\partial x^2} dx + EI_y \int_{L-l_w}^{L} \frac{(L-x)}{l_w} \cdot \frac{\partial^2 \varphi_i(x)}{\partial x^2} \cdot \frac{\partial^2 \varphi_j(x)}{\partial x^2} dx \quad (23)$$

$$m_{ij} = \rho S \int_0^{L-l_w} \varphi_i(x) \cdot \varphi_j(x) dx + \rho S \int_{L-l_w}^{L} \frac{(L-x)}{l_w} \cdot \varphi_i(x) \cdot \varphi_j(x) dx \quad (24)$$

where l_w= 72μm is the height of the wedge tip on the x axis. So if the first flexural frequency of the cantilever is known, the thickness of the cantilever can be calculated by the modified (22) (set m=0). In the experiments, three cantilevers are characterized and the results are shown in the Table I, in which the length and width of the cantilever are measured as 600μm and 140μm for the stiffness calculation. The experimental results show that the fabrication errors of AFM cantilever leads to great differences between the measured parameters and commercially provided ones. This indicates the necessary of the calibration of cantilevers to the accurate applications.

In the following experiments, the no.1 cantilever is selected, which is mounted on the micromanipulator (3 DOF coarse positioning stages and 1 DOF piezo-actuated nanopositioning stage).

TABLE I
CALIBRATION RESULTS OF THREE CANTILEVERS

Descriptions	Cantilever No.1	Cantilever No.2	Cantilever No.3
Res. Freq.(kHz)	38.75	42.45	46.69
Thickness (μm)	9.194	10.072	11.078
Stiffness(N/m)	20.15	26.48	35.25

C. Mass Sensitivity of First Three Modes

The flexural and torsional vibrations of microcantilever are detected by a laser beam and a four-quadrant photo detector with a lock-in amplifier. Each of the first three modal frequencies is examined separately with 1 Hz interval sweeps between the half magnitude frequency points. Indeed, it is possible to carefully position the laser spot near the edge of the microcantilever so as to maximize the contribution of torsional mode. After carefully preparing the experimental system, a Ragweed Pollen with a diameter of 20μm is mounted on the free end of the test microcantilever as in Fig. 3(a) to purposefully bias the torsional modal frequency and the experiment was rerun to determine a set of modal frequencies. In order to get a high sensitivity, the Ragweed Pollen is located on the edge of the test microcantilever near the free end as in Fig. 3(b). Under an optical microscopy with a resolution of 0.55μm/pixel, the position of the Ragweed Pollen measured as (519, -77) (μm) in the given coordinate as in Fig. 2. The first three resonant frequencies without and with this added mass

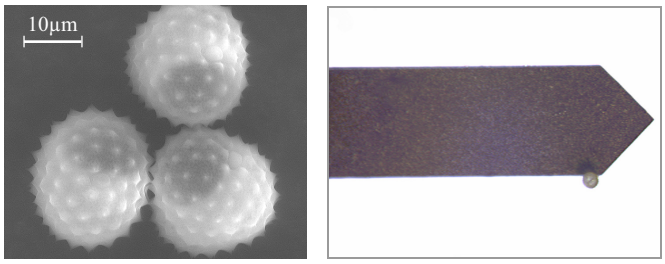

(a) (b)

Fig.3. (a) SEM image of Ragweed pollen with a diameter of 20μm. (b) An optical image of the microcantilever with an attached Ragweed Pollen.

are recoded. From the Fig.4, we can get the frequency shifts of the first three modes are 140Hz, 700Hz and 2.4 kHz, respectively, which indicates that the first torsional mode has relative highest sensitivity of mass detection because of the higher torsional stiffness of microcantilever. The second flexural mode also has a high sensitivity, because normally the higher flexural mode has higher sensitivity because of the smaller effective mass of the microcantilever [21].

As shown in Table II, using these three modes the average mass of the Ragweed Pollen is measured as 3.838×10^{-12} kg under a humidity of 60%, which is quite accord with the previous experimental result [27].

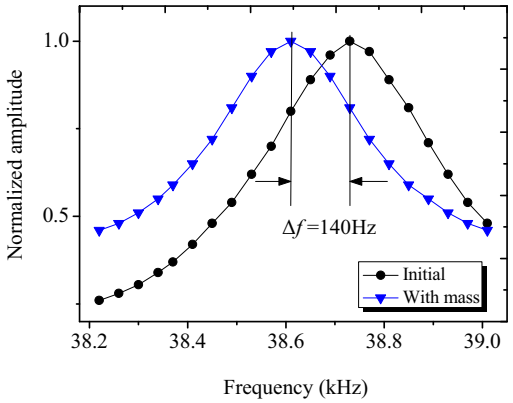

(a)

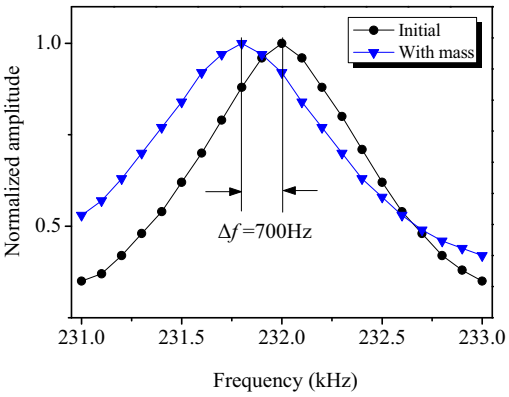

(b)

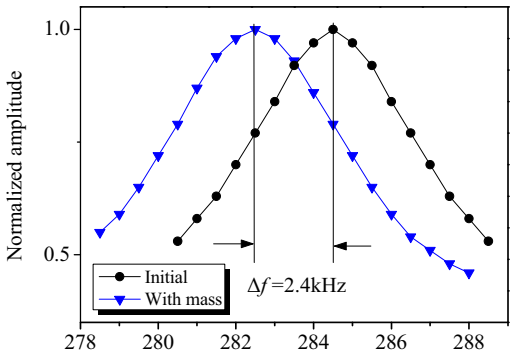

(c)

Fig.4. Frequency shift in spectrum after the Ragweed Pollen has been loaded. (a) Shift under the first flexural mode. (b) Shift under the second flexural mode. (c) Shift under the first torsional mode.

TABLE II
MASS DETECTION RESULTS USING THE FIRST THREE MODES

Descriptions	1st flexural	2ed flexural	1st torsional	Average
Mass(10^{-12}kg)	3.795	3.879	3.848	3.841

In the torsional vibration experiments, the natural frequency of the "cantilever-object" system is measured using asinusoidal excitation with a very low magnitude, because the micro-object easily escapes from the end-effecter with a high frequency (the first torsional resonant frequency of the cantilever is 284.7 kHz). The experimental results show that the torsional resonant frequencies of the system strongly depend on the attaching positions of the microsphere. In order to validate the relationship among the resonant frequencies, attaching position and mass of the microsphere, as shown in Figure 5, an ragweed pollen is located on 4 different positions by a AFM tip along the *y* axis. As shown in the (21), the nature frequency is determined by the position on *x*, *y* axis and mass of the ambrosia pollen. This problem is resolved as follows: firstly, the microscopic vision is also employed to measure the positions, which has a magnification of 20× and a resolution of 0.55μm/pixel. Secondly detect the first torsional resonant frequency of the "cantilever-object" system, and then using the proposed method to calculate the mass of the ambrosia pollen.

The corresponding experimental results are shown in Table III. Note that the measurement results will be more imprecise when the adhering position is approaching the torsional axis of microcantilever, which is in accordance with the analysis mentioned in the last part.

D. Multi-Mass Detection of Ragweed Pollens

Fig.6 shows that four same ragweed pollens adhered to the back surface of the cantilever with different positions. The positions are measured by microscopic vision with a resolution of 0.55μm/pixel. The experimental results are shown in Table IV. The mass 3.905×10^{-12} kg is calculated by the pro

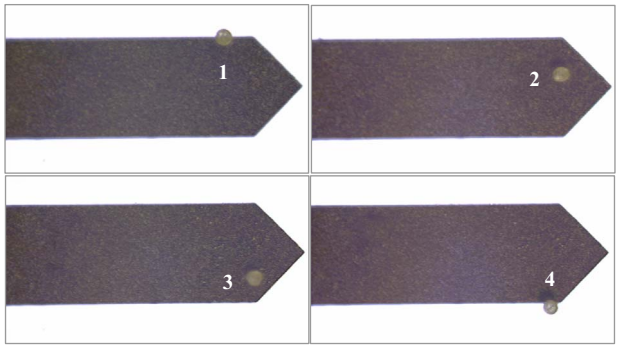

Fig.5. An ambrosia pollen is placed on four different positions along the transversal coordinate of microcantilever.

TABLE III
THE MASS DETECTION OF THE AMBROSIA POLLEN ADHERED TO THE CANTILEVER ON DIFFERENT POSITION.

Ambrosia pollen	Positions (*x*, *y*) (μm)	1 st torsional res. freq. (kHz)	Gross Mass (10^{-12}kg)
1	(491, 68)	282.9	3.829
2	(536,17)	284.6	2.984
3	(530, -38)	284.1	3.816
4	(519, -77)	282.3	3.848

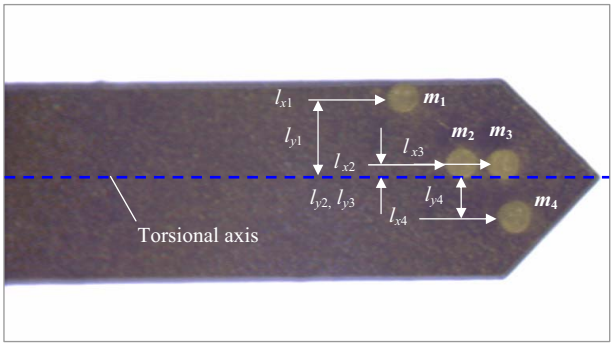

Fig.6. Four ragweed pollens adhered to the cantilever with different positions. The positions are measured by the microscopic vision with a resolution of 0.55μm/pixel.

TABLE IV
THE RESULTS OF MULTI-MASS DETECTIONG OF THE AMBROSIA POLLEN

Ambrosia pollens	Positions (l_{xn}, l_{yn}) (μm)	1 st torsional res. freq. (kHz)	Mass (10^{-12}kg)
1	(461, 55)	281.9	3.905
2	(509, 10)		
3	(532, 10)		
4	(540, -28)		

posed method, which is a litter higher than the real mass of the ragweed pollen. Two reasons contributes to this error, the first one is the resolution of the signal generator, which is 100Hz in this range, and the second reason is that two ragweed pollens m_2 and m_3 near the torsional axis of the microcantilever,

which induce the imprecision of the whole detection. This is the disadvantage of the mass detection using the torsional mode. However, in contrast with the conventional flexural mode, the first torsional mode has higher mass sensitivity if the mass is located near the edge of the free end of microcantilever, which promises the possibility of using ordinary microcantilevers for the higher sensitivity in the bio/chemical molecular detection.

IV. Conclusion

In order to achieve a higher-sensitivity mass detection, a model for the first torsional mode of the "cantilever-object" system based on the Rayleigh–Ritz theory is developed. An experimental micromanipulator with an active end-effector is developed, and ragweed pollens with a diameter of 20μm are used as the attaching mass in the experiments. An ragweed pollen is mounted on the edge of free end of microcantilever to purposefully compare the mass sensitivities of the first three modes of microcantilever. The experimental results show that the mass sensitivity of the first torsional mode is an order of magnitude greater than the first flexure mode, and also much higher than the second resonant mode. In order to verify the effect of positions on the sensitivity of the first torsional mode, an ambrosia pollen is placed on four different positions on the transverse axis near the cantilever tip and the experimental results indicate that when the ambrosia pollen near the edge of the cantilever, fine calculating results can be obtained comparing the results measured by the microscopic vision, but near the torsional axis, the results are not ideally accurate, which conform to the model analysis. In the multi-mass detection, four ragweed pollens are located on the cantilever and the microscopic vision is employed to measure the positions of the ragweed pollens on the longitudinal and transversal axis of the microcantilever.

In conclusion, the higher resonant modes of the microcantilever can achieve higher mass sensitivity, besides using the high sensitive microcantilever, which provides a promising method to detect the smaller objects using the ordinary microcantilevers. Using microscopic vision or other methods for the measurement of the attaching positions and the models considering the attaching position of the mass, more precise detection results can be easily obtained.

Acknowledgment

This work has been partially supported by European project NANORAC (Contract number: STRP 013680).

References

[1] G. Binning, C. F. Quate and C. Gerber, "Atomic force microscope," *Phys. Rev. Lett.*, vol. 56, pp. 930–3, 1986.

[2] J. P. Cleveland and S. Manne, "A nondestructive method for determining the spring constant of cantilevers for scanning force microscopy," *Rev. Sci. Instrum*, vol. 64, pp. 403–5, 1993.

[3] G. Abadal, Z. J. Davis, B. Helbo, X. Borrise, R. Ruiz, A. Boisen, F. Campabadal, J. Esteve, E. Figueras, F. Perez-Muranoand N. Barniol "Electromechanical model of a resonating nano-cantilever-based sensor for high-resolution and high-sensitivity mass detection," *Nanotechnology*, vol. 12, pp. 100–4, 2001.

[4] Z. J. Davis, G. Abadal, O. Kuhn, O. Hansen, F. Grey and A. Boisen, "Fabrication and characterization of nanoresonating devices for mass detection," *J. Vac. Sci. Technol.,* vol. 18, pp. 612-616, 2000.

[5] V. N. Lavrik and P. G. Datskos, "Femtogram mass detection using photothermally actuated nanomechanical resonators," *Appl. Phys. Lett.,* vol. 82, pp. 2697-2699, 2003.

[6] B. Ilica, H. G. Craighead, S. Krylov, W. Senaratne, C. Ober and P. Neuzil, "Attogram detection using nanoelectromechanical oscillators," *J App. Phys.,* vol. 95, pp. 3694–3703, 2004.

[7] J. L. Arlett, J. R. Maloney, B. Gudlewski, M. Muluneh and M. L. Roukes, "Self-Sensing Micro- and Nanocantilevers with Attonewton-Scale Force Resolution," *Nano Lett.,* vol. 6, pp. 1000-1006, 2006.

[8] S. Hosaka, T. Chiyoma, A. Ikeuchi, H. Okano, H. Sone and T. Izumi, "Possibility of a femtogram mass biosensor using a self-sensing cantilever," *Current Applied Physics,* vol. 6, pp. 384–388, 2006.

[9] Z. Y. Shen, W. Y. Shih and W. H. Shih, "Self-exciting, self-sensing $PbZr_{0.53}Ti_{0.47}O_3/SiO_2$ piezoelectric microcantilevers with femtogram/Hertz sensitivity," *Appl. Phys. Lett.,* vol. 89, pp. 023506, 2006.

[10] M. Su, S. Y. Li and V. P. Dravid, "Microcantilever resonance-based DNA detection with nanoparticle probes," *Appl. Phys. Lett.,* vol. 82, pp.3562–3564, 2003.

[11] B. Ilic, D. Czaplewski, M. Zalalutdinov and H. G. Craighead, "Single cell detection with micromechanical oscillators," *J. Vac. Sci. Technol.,* vol. B19, pp. 2825–2828, 2001.

[12] A. Gupta, D. Akin and R. Bashir, "Single virus particle mass detection using microresonators with nanoscale thickness," A*ppl. Phys. Lett.,* vol. 84, pp. 1976-1978, 2003.

[13] A. Gupta and D. Akin,"Detection of bacterial cells and antibodies using surface micromachined thin silicon cantilever resonators," *J Vac. Sci. Technol.,* vol. B22, pp. 2785-2791, 2004.

[14] A. Vidic, D. Then and C. H. Ziegler, "A new cantilever system for gas and liquid sensing," *Ultramicroscopy,* vol. 97, pp. 407–416, 2003.

[15] C. Hagleitner, A. Hierlemann, D. Lange, A. Kummer, N. Kerness, O. Brand and H Baltes, "Smart single-chip gas sensor microsystem," *Nature,* vol. 414, pp. 293-296, 2001.

[16] M. Spletzer, A. Raman, A. Q. Wu and X. F. Xu, "Ultrasensitive mass sensing using mode localization in coupled microcantilevers," A*ppl. Phys. Lett.*, vol. 88, pp. 254102, 2006.

[17] S. Haliyo, S. Régnier and J. C. Guinot, "[*mü*] MAD, the adhesion based dynamic micromanipulator," *European J. Mechanics A/Solids*, vol. 22, pp. 903–916, 2003.

[18] M. Nishio, S. Sawaya, S. Akita and Y. Nakayama, "Carbon nanotube oscillators toward zeptogram detection," A*ppl. Phys. Lett.* vol. 86, pp. 133111, 2005.

[19] L. B. Sharos , A. Raman, S. Crittenden and R. Reifenberger, "Enhanced mass sensing using torsional and lateral resonances in microcantilevers," *Appl. Phys. Lett.,* vol. 84, pp. 4638-4640, 2004.

[20] Søren Dohn,a, Rasmus Sandberg, Winnie Svendsen, and Anja Boisen, " Enhanced functionality of cantilever based mass sensors using higher modes," *Appl. Phys. Lett.,* vol. 85, pp. 233501, 2005.

[21] D. Z. Jin, X. X. Li, J. Liu, G. M. Zuo, Y. L. Wang, M. Liu and H. T. Yu, "High-mode resonant piezoresistive cantilever sensors for tens-femtogram resoluble mass sensing in air," *J. Micromech. Microeng.,* vol. 16, pp. 1017-1023, 2006.

[22] D. J. Gorman, *Free vibration analysis of beams and shafts*, New York: Wiley, 1975.

[23] C. T. F. Ross, *Finite element programs for structural vibrations*, London: Springer-Verlag, 1991.

[24] A. W. Leissa, "The historical bases of the Rayleigh and Ritz methods," *J. Sound Vib.*, vol. 287, pp. 961–978, 2005.

[25] N. A. Burnham, X. Chen, C. S. Hodges, G. A. Matei, E. J. Thoreson, C. J. Roberts, M. C. Davies and S. J .B. Tendler, "Comparison of calibration methods for atomic-force microscopy cantilevers," *Nanotechnology, vol.* 14, pp. 1–6, 2003

[26] D. A. Mendels, M. Lowe, A. Cuenat, M. G. Cain, E. Vallejo, D. Ellis and F. Mendels, "Dynamic properties of AFM cantilevers and the calibration of their spring constants," *J. Micromech. Microeng*., vol. 16, pp. 1720–1723, 2006.

[27] James B. Harrington, JR. and Kurt Metzger, "Ragweed Pollen Density," *American Journal of Botany*, vol. 50, no. 6, Part 1, pp. 532-539, 1963.